Citation: Molecular Therapy — Methods & Clinical Development (2014) **1,** 14038; doi:10.1038/mtm.2014.38

www.nature.com/mtm

ARTICLE

Adeno-associated viral vectors do not efficiently target muscle satellite cells

Andrea LH Arnett[1–3,7], Patryk Konieczny[2,8], Julian N Ramos[2,3], John Hall[2], Guy Odom[2], Zipora Yablonka-Reuveni[4], Joel R Chamberlain[5] and Jeffrey S Chamberlain[2,6]

Adeno-associated viral (AAV) vectors are becoming an important tool for gene therapy of numerous genetic and other disorders. Several recombinant AAV vectors (rAAV) have the ability to transduce striated muscles in a variety of animals following intramuscular and intravascular administration, and have attracted widespread interest for therapy of muscle disorders such as the muscular dystrophies. However, most studies have focused on the ability to transduce mature muscle cells, and have not examined the ability to target myogenic stem cells such as skeletal muscle satellite cells. Here we examined the relative ability of rAAV vectors derived from AAV6 to target myoblasts, myocytes, and myotubes in culture and satellite cells and myofibers *in vivo*. AAV vectors are able to transduce proliferating myoblasts in culture, albeit with reduced efficiency relative to postmitotic myocytes and myotubes. In contrast, quiescent satellite cells are refractory to transduction in adult mice. These results suggest that while muscle disorders characterized by myofiber regeneration can be slowed or halted by AAV transduction, little if any vector transduction can be obtained in myogenic stems cells that might other wise support ongoing muscle regeneration.

Molecular Therapy — Methods & Clinical Development (2014) **1**, 14038; doi:10.1038/mtm.2014.38; published online 17 September 2014

INTRODUCTION

Adeno-associated virus (AAV) is a small, single-stranded DNA parvovirus that has featured prominently in the field of gene therapy. Recombinant AAV (rAAV) is a promising therapeutic candidate for use in gene replacement strategies due to encouraging results in numerous animal models of genetic disease and in human clinical trials. Unlike the wild-type virus, recombinant AAV vectors lack the viral genes that promote integration, and thus persist almost entirely in episomal form within transduced tissues.[1–3] This feature of rAAV biology contributes to the safety profile of the vector by reducing the risk of deleterious integration near oncogenes and in germ cells.[4,5]

Numerous primate serotypes and over 100 AAV variants have been isolated, many of which exhibit unique patterns of tissue tropism and transduction.[6] The transduction profile of several of these vectors has been extensively compared in multiple studies, and a high degree of tropic variability has been observed between serotypes. For example, rAAV8 and rAAV9 have been shown to achieve high levels of hepatocyte transduction,[7,8] whereas rAAV1 and rAAV5 perform effectively within the central nervous system.[9–12] In striated muscle, high transduction levels have been attained using rAAV1, 6, 7, 8, and 9 (refs. 8,13–19). In particular, rAAV6 is strongly tropic for striated muscle and has demonstrated the highest efficiency of cardiac transduction among rAAV serotypes 1–9 (refs. 13–16). Thus, rAAV6 is a candidate for treatment of a large number of genetic disorders related to skeletal and cardiac muscle.

The muscular dystrophies comprise a heterogeneous group of genetic disorders affecting striated muscle. The most common of the dystrophies is Duchenne muscular dystrophy (DMD), a lethal X-linked recessive disorder affecting ~1 in every 3,500 live male births.[20] DMD is characterized by progressive and debilitating wasting of striated muscle, culminating in cardiac and respiratory failure by the third decade of life. At this time, no curative treatment exists, and high-dose corticosteroids remain the primary component of the majority of established treatment regimens.[21] DMD is caused by mutations in the gene encoding for dystrophin. The full-length isoform of dystrophin is a structural protein that localizes to the sarcolemma of myofibers and serves to stabilize the muscle membrane during periods of mechanical stress.[20] In the absence of dystrophin, muscles are highly susceptible to contraction-induced injury and are repeatedly damaged during normal use.[22–25] This leads to a chronic cycle of necrosis and regeneration that ultimately results in widespread fibrosis and deposition of adipose tissue.

The first three authors contributed equally to this work.

[1]Medical Scientist Training Program, University of Washington School of Medicine, Seattle, Washington, USA; [2]Department of Neurology, University of Washington School of Medicine, Seattle, Washington, USA; [3]Molecular and Cellular Biology Program, University of Washington School of Medicine, Seattle, Washington, USA; [4]Department of Biological Structure, University of Washington School of Medicine, Seattle, Washington, USA; [5]Department of Medicine, University of Washington School of Medicine, Seattle, Washington, USA; [6]Department of Biochemistry, University of Washington School of Medicine, Seattle, Washington, USA; [7]Current Address: University of California at San Francisco, Fresno Center for Medical Education and Research, Fresno, California, USA; [8]Current Address: Institute of Molecular Biology and Biotechnology, Adam Mickiewicz University, Poznan, Poland. Correspondence: JS Chamberlain (jsc5@uw.edu)

Received 15 April 2014; accepted 7 July 2014

The successful use of rAAV to treat DMD depends on efficient transduction of muscle tissue in a proinflammatory, dystrophic environment. Histologically, dystrophic muscles are characterized by a chronic inflammatory cell infiltrate and a heterogeneous combination of myofibers at various stages of degeneration and regeneration.[20] Activated and proliferating muscle progenitor cells can be observed in response to a high degree of dystrophic turnover. While it has been clearly demonstrated that rAAV6 can transduce mature myofibers *in vivo*,[13,14,16] the transduction efficiency of muscle precursor cells (MPCs) and immature myotubes has not been characterized. The capacity to target MPCs is an important aspect to consider in the development of any gene replacement strategy for the muscular dystrophies, as transduced MPCs could potentially serve to replenish myofibers that are lost during normal fiber turnover.

In the following studies, we evaluated the capacity of rAAV6 to transduce both MPCs and myofibers in *wt* and *mdx* mice. The *mdx* mouse demonstrates many of the pathological features of DMD and serves as a well-established genetic model for this disease.[26] Our results demonstrate that rAAV6 does not effectively transduce muscle satellite cells, but preferentially transduces differentiated myofibers, both *in vitro* and *in vivo*.

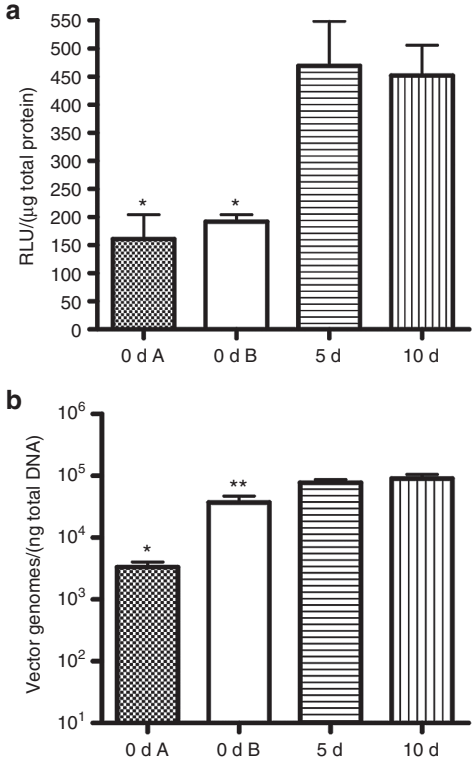

Figure 1 rAAV6 transduction of myotubes is more efficient that myoblast transduction *in vitro*. MM14 myoblasts or myotubes were transduced with rAAV6-CMV-AP, and both AP expression (**a**) and vector genome number (**b**) were quantified. Myoblasts were incubated with vector for either 1 hour *(0d A)* or 3 days *(0d B)* subsequent to withdrawal of FGF-2 and serum to halt proliferation. Shortened exposure to vector did not result in a statistically significant decrease in transduction. Myotubes were transduced at either 5 days *(5d)* or 10 days *(10d)* post-differentiation. Myotubes transduction at either timepoint was significantly increased compared to myoblasts. * indicates significantly different compared to 5d and 10d cohorts. ** indicates significantly different in comparison to 10 day cohort only. $P < 0.05$. FGF, fibroblast growth factor.

RESULTS

rAAV6 transduces myotubes more efficiently than myoblasts in culture

The MM14 cell line is an immortalized mouse myoblast line that has been extensively utilized to study skeletal muscle myogenesis.[27–30] When grown in appropriate culture conditions, including serum and fibroblast growth factor (FGF-2) supplementation, MM14 myoblasts proliferate and remain in a mononuclear state. Serum depletion and withdrawal of FGF-2 induces withdrawal from the cell cycle and terminal differentiation into myocytes and myotubes within a few days of induction.[27,28,31]

We independently evaluated rAAV6 transduction of myoblasts and myotubes *in vitro* utilizing an alkaline phosphatase (AP) reporter (Figure 1). Serum and FGF-2 were withdrawn from proliferating myoblasts and rAAV6-CMV-AP (3×10^9 vector genomes per well in 1 ml of media) was added to the culture media. Cells were harvested 3 days post-transduction, and reporter expression and vector genomes (vg) were quantified via a chemiluminescence assay (Figure 1a) and by quantitative-polymerase chain reaction (QPCR) (Figure 1b), respectively. An additional cohort of myoblasts was incubated with vector for a shorter duration of time (1 hour), at which point the media was exchanged and maintained until the 3-day endpoint. Interestingly, shortened exposure to vector was not associated with a statistically significant decrease in transduction, suggesting that the majority of transduction-competent vector particles are taken up by the cells within the first hour in culture. This is consistent with previous reports demonstrating rapid uptake of rAAV particles in cultured fibroblasts.[32]

A similar transduction protocol was evaluated in maturing myotubes. Differentiation was induced via withdrawal of serum and FGF-2, and cells were transduced at either 5 or 10 days postinduction. As described above, cells were harvested for analysis 3 days post-transduction. We observed a significant increase in transduction of differentiating MM14 myotubes in comparison to myoblasts. In contrast, there was no significant difference in transduction between cultures transduced at 5 versus 10 days postdifferentiation. This implies that modulation of transduction efficiency occurs early in the differentiation process, prior to 5 days postinduction.

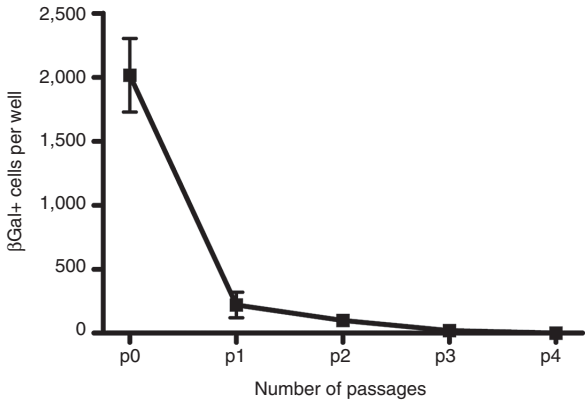

Figure 2 Vector-mediated reporter expression is diminished under conditions of high myoblast proliferation and turnover. C2C12 myoblasts were transduced with rAAV6-CMV-βGal at an MOI of 100. Cells were serially passaged every 2 days and diluted 1:10 with each passage. 90% of the population was discarded with each passage. At each passage, a cohort of wells ($n = 2$) was stained for βGal expression and the number of positive cells was quantified. Myoblasts gradually lost reporter expression over multiple cycles of dilution and proliferation. After four passages, the number of positive cells was reduced to ~2 per well. MOI, modality of infection.

Vector-mediated reporter expression is diminished under conditions of myoblast proliferation and turnover

rAAV vectors integrate only at very low frequencies,[5] and thus, vector-mediated transgene expression is predicted to diminish over time under conditions of ongoing cellular proliferation and turnover. Cells were transduced with rAAV6-CMV-*lac*Z at an modality of infection (MOI) of 100. This MOI was sufficient to induce visually detectable levels of β-galactosidase (βGal) expression in nearly all cells, whereas an MOI of 50 resulted in ~60% of cells staining positively for βGal (data not shown). Transduced cells were passaged and diluted 1:10 every 2 days (90% of the population was discarded with each passage) (Figure 2). Prior to each passage, a subset of wells was stained for βGal expression, and the total number of positive cells was quantified. We observed an ~90% decrease in the total number of positive cells following a single cycle of proliferation and dilution. This loss was less dramatic at subsequent passages, but the total number of positive cells continued to decline. After four passages, only a few cells stained positive for βGal expression. These results confirm that rAAV6-mediated transgene expression is negatively impacted by cellular turnover in cultured myoblasts.

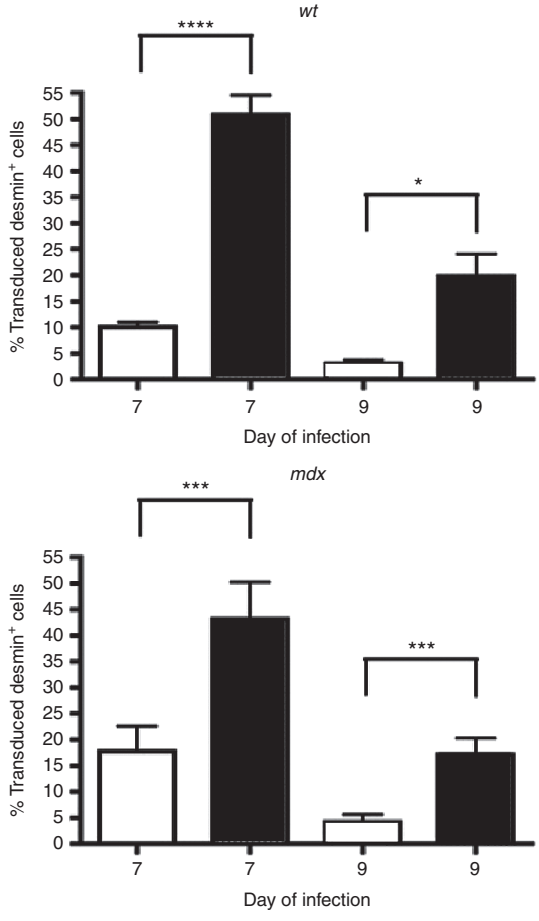

Figure 3 *In vitro* rAAV6-mediated transduction of single myofiber cultures reveals a marked preference for multinucleated muscle cells. Single myofibers from both *wt* (top) or *mdx* (bottom) mice were isolated and cultured to establish a mixed population of mononuclear muscle progenitor cells and multinuclear myotubes. Cultures were transduced with rAAV6-mCherry on either day 7 or day 9. Cells were stained for desmin expression 2 days post-transduction, and the number of cells coexpressing both desmin and mCherry was quantified. Multinucleated muscle cells (dark bars) were preferentially targeted at both transduction timepoints relative to mononuclear cells (white bars). In cultures transduced on day 9, the total number of desmin-positive cells was reduced, but the proportion of myofiber transduction increased. $^{*}P < 0.05$; $^{***}P < 0.01$; $^{****}P < 0.001$.

rAAV6 transduction of single-fiber cultures reveals a marked preference for multinucleated muscle cells and mature myofibers

To investigate transduction of MPCs and myofibers, we isolated single, intact myofibers from both *wt* and *mdx* mouse muscles (Figure 3). Fibers were cultured to stimulate proliferation and differentiation of resident satellite cells on the isolated fibers, and cultures were maintained briefly in proliferation media prior to induction of differentiation, as previously described.[33] Single myofibers cultured in this manner produce a mixed population of mononuclear activated satellite cells and myoblasts and multinucleated myotubes. Thus, single fiber cultures can be utilized to investigate the *in vitro* tropism of rAAV6 in a mixed population of MPCs and myofibers.

Fiber cultures were transduced with rAAV6-CMV-mCherry following either 7 or 9 days in culture and fixed for immunofluorescent staining 48 hours post-transduction. The total number of transduced muscle cells was quantified and subdivided into mononuclear and multinuclear components. Positivity was defined as coexpression of mCherry and the muscle-specific marker, desmin. Both transduction timepoints revealed a significant bias toward transduction of multinucleated muscle cells (Figure 3). Similar trends were observed in both *mdx* and *wt* fiber cultures, indicating that transduction bias towards multinucleated muscle cells is independent of dystrophin expression.

Transduction efficiency is reduced during the proliferative phase of skeletal muscle regeneration

In skeletal muscle, the regenerative response to injury is characterized by an inflammatory response and satellite cell activation, followed by a rapid increase in myoblast proliferation.[34–38] Within a few days postinjury, MPCs fuse to regenerate damaged myofibers, and normal muscle architecture is gradually restored during the process of fiber maturation. Thus, the early stages of muscle regeneration present an opportunity to evaluate rAAV6 transduction of skeletal muscle during a period of high myoblast proliferation and myofiber formation *in vivo*.

We employed a notexin (NTX)-induced injury model, which was previously shown to destroy the majority of muscle fibers and induce generation of fibers *de novo* in the extensor digitorus longus (EDL) muscle of the hindlimb[39] and evaluated the efficiency of muscle transduction following sequential, timed injections of rAAV6 at different stages post-NTX treatment (Figure 4). Mice received an intramuscular (IM) injection of NTX into EDL, followed by IM injection of rAAV6-CMV-AP (1×10^{10} vg) at either 2, 3, 4, or 5 days postinjury. Muscles were harvested at 2 weeks postinjection of rAAV6 and stained for AP expression (Figure 4a). In addition, vector genomes were quantified via QPCR (Figure 4b). We observed a progressive increase in transduction efficiency as the interval between injury and AAV injection increased. AAV injection 2 days postinjury resulted in minimal transduction and a mosaic pattern of AP expression. In contrast, AAV injection 4 days postinjury resulted in an approximately fivefold increase in transduction compared to the initial 2-day timepoint, and a more even distribution of AP expression. This correlates with the timing of fusion of proliferating myoblasts and myofiber formation, which have been shown to occur 3–4 days postinjury[39,40] (unpublished data). Transduction increased approximately ninefold when the interval between injury

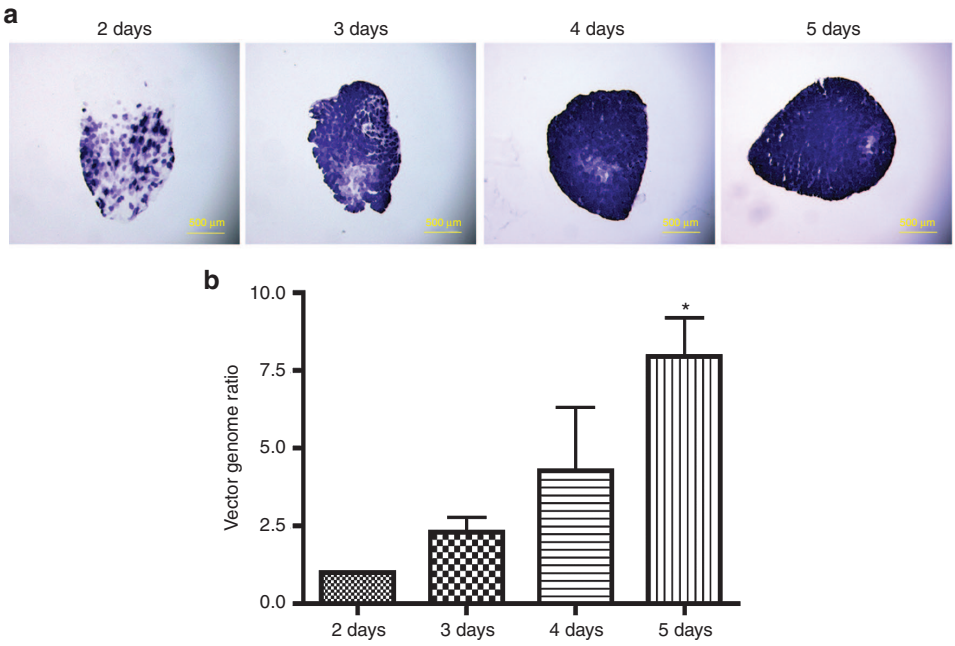

Figure 4 rAAV6 transduction efficiency is reduced during the early proliferative and inflammatory phase of muscle regeneration. Mice ($n = 3$) received an intramuscular (IM) injection of notexin in the extensor digitorus longus muscle, followed by rAAV6-CMV-AP injection at 2, 3, 4, or 5 days postinjury. Muscles were collected 2 weeks following rAAV6 injection and evaluated for AP expression (**a**) and vector genomes (**b**). We observed a trend towards increased transduction efficiency that correlated with an increase in the interval between injury and rAAV6 injection. Vector genome ratio is reported relative to copy number at the earliest injection timepoint (2 days).

and rAAV6 injection was increased to 5 days. These data are consistent with our *in vitro* results indicating that myofibers are more efficiently targeted than myoblasts, and suggests that the rate of myoblast proliferation and myofiber formation may limit the efficiency of rAAV6 in regenerating muscle. Once the myofibers were formed, no significant change in the transduction efficiency was observed when compared to uninjured muscles, suggesting that the process of fiber maturation does not adversely affect transduction efficiency.

rAAV6 does not effectively transduce satellite cells *in vivo*

We employed three strategies to evaluate transduction of skeletal muscle satellite cells *in vivo*. Our initial experiment was performed using both wt and *mdx* nestin enhanced green fluorescent protein (eGFP) mice. These latter mice express a eGFP reporter under control of the nestin promoter, which is active in quiescent satellite cells.[41,42] Mice received bilateral IM injections of rAAV6-CMV-mCherry (1×10^{10} vg) in the EDL muscle. Approximately 50 fibers were isolated from both *wt* and *mdx* muscles 4 weeks postinjection and cultured as described above. Of these myofibers, ~80% were positive for mCherry. Coexpression of eGFP and mCherry was not observed in any satellite cell (*e.g.*, Figure 5a). This observation held true irrespective of whether the originating myofiber was positive or negative for mCherry expression. Instead, eGFP-positive/mCherry-negative satellite cells were observed to migrate from isolated fibers and initiate proliferation and differentiation (Figure 5b,c). None of the derived mononuclear cells and myotubes became positive for mCherry expression, with the exception of myotubes that fused with the originally plated mCherry positive fiber (Figure 5c, inset).

To expand our analysis to a larger population of satellite cells and other MPCs, we injected the tibialis anterior (TA) of *wt* mice with rAAV6-CMV-eGFP (1×10^{11} vg) and isolated MPCs and mononuclear cells from the entire muscle at 4 weeks postinjection. Approximately 3×10^5 mononuclear cells were isolated and sorted for GFP expression via FACS (Supplementary Figure S1a). Of these, ~13% were positive for eGFP expression (Supplementary Figure S1b). The entire eGFP-positive population was plated under myogenic differentiation conditions, and cultures were tracked for 4 days. A total of four myogenic colonies were identified within the sorted population, but none of these colonies expressed eGFP. In parallel, ~4×10^5 cells were directly plated without sorting. The unsorted population of cells generated a large number of myogenic colonies, but none of these were found to originate from eGFP-positive cells.

It is unclear if satellite cells and MPCs did not express eGFP because they were not transduced after injection or if the episomal vector genome was lost through proliferation prior to differentiation in culture. To address this question, we sought to monitor vector transduction and quantify vector genomes directly in satellite cells. We initially examined cross-sections from rAAV6-injected *wt* and *mdx* muscles for rAAV transduction. As above, mice received bilateral IM injections of rAAV6-CMV-GFP (1×10^{11} vg) in the TA. Muscles were harvested 4 weeks postinjection, fixed, sectioned, and stained for Pax7,[41,43] which is expressed in quiescent satellite cells (Figure 6a). Consistent with our previous results, no Pax7-positive cells were found to coexpress eGFP in either *wt* (Figure 6a) or *mdx* (not shown) muscles (in ~150 satellite cells per cohort). These results reveal a lack of satellite cell transduction *in vivo* and indicate that rAAV6 preferentially targets myofibers in adult skeletal muscle.

To determine the presence of vector genomes in satellite cells *in vivo*, TA and EDL muscles of both *wt* and *mdx* mice were injected with rAAV6-CMV-mCherry. At 4 weeks postinjection, injected muscles were harvested and either directly imaged for mCherry fluorescence or used for satellite cell isolation by MACS (Figure 6b,c).[44] DNA extracted from isolated satellite cells as well as whole muscle was measured by quantitative PCR. No significant level of rAAV DNA was detected in satellite cells from either strain. However, vector

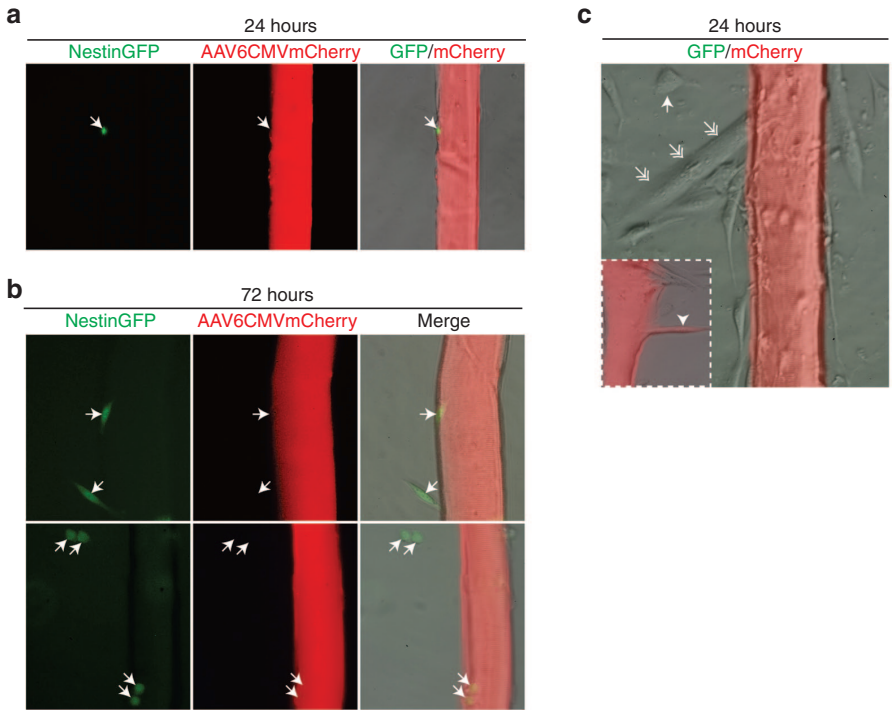

Figure 5 Single fiber cultures from nestin-GFP mice injected with rAAV6. Mice received an intramuscular (IM) injection of rAAV6-CMV-mCherry in the extensor digitorus longus muscle. Fibers were isolated from injected muscles 4 weeks post-transduction and cultured for up to 6 days. At 24 hours, nestin/eGFP-positive satellite cells could be visualized on myofibers, but no cells stained for both eGFP and mCherry (**a**). eGFP-positive, mCherry-negative satellite cells were tracked as they migrated from the parent fibers and established myogenic colonies (**b**). Satellite cells remained negative for mCherry expression. By 6 days, numerous myotubes had formed in the cultures from the proliferating and terminally differentiating myoblasts (**c**), but the only eGFP-positive myotubes observed were those that had fused with the original myofiber (**c**, inset). eGFP, enhanced green fluorescent protein.

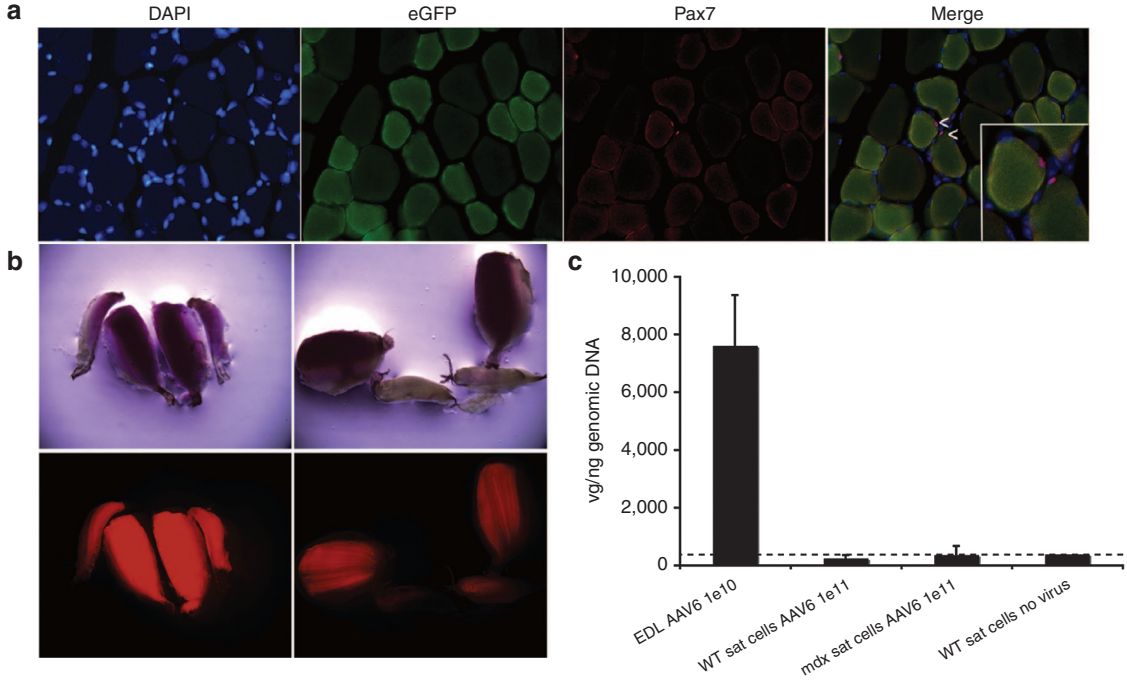

Figure 6 Analysis of satellite cell transduction in muscles injected with rAAV6. (**a**) Cross-sections of wild-type muscles injected with rAAV6-CMV-eGFP (**a**). Injected muscles were collected 4 weeks postinjection and stained for Pax7 and DAPI, then visualized under a fluorescence microscope. eGFP expression was not observed in any Pax7-positive cells. (**b,c**) Both *wt* and *mdx* mice were injected with rAAV6-CMV-mCherry with the dose indicated in (**c**). The high level of transduction using the 1×10^{10} vg dose was evident upon harvesting the muscles (**b**) (images taken at 7× magnification). No vector genomes were detected among satellite cells of either mouse strain 4 weeks postinjection (**c**). However, vector genomes were detected in DNA extracted from whole, injected extensor digitorus longus muscles (**c**). DAPI, 4′,6-diamidino-2-phenylindole; eGFP, enhanced green fluorescent protein.

genomes were detected in DNA extracted from whole injected EDL muscles (Figure 6c). Together, these data indicate that AAV vector genomes do not target satellite cells despite the widespread transduction apparent upon gross muscle dissection (Figure 6b).

In addition to rAAV6, vectors derived from AAV8 and 9 have emerged as promising vectors for muscle transduction.[8,16,17] To examine whether vectors pseudotyped with AAV8 or 9 capsids could target satellite cells we injected rAAV6, 8, or 9 vectors expressing CMV-eGFP into the TA muscles of wild-type mice. In other studies, we have observed that rAAV6 gives higher levels of transduction when intramuscularly injected into mouse muscles (unpublished data). Also, since we had already established that rAAV failed to transduce satellite cells, we injected ~40-fold higher levels of rAAV8 and 9 than rAAV6. All three vector types efficiently transduced myofibers, as expected (Figure 7). By costaining with Pax7 and laminin, we were able to identify satellite cells in each cohort. As before, we saw no Pax7$^+$/eGFP$^+$ cells when using rAAV6 nor did we observe positive satellite cells with rAAV9 (Figure 7). With rAAV8, we did observe rare Pax7$^+$/eGFP$^+$ satellite cells, but they represented less than 5% of the observed satellite cells in the injected muscles. Interestingly, either due to injection site trauma or perhaps toxicity of eGFP expression, we observed areas of regenerating myofibers in the rAAV6-injected muscles. In these regions, we found rare Pax7-negative/eGFP$^+$ cells between the basal lamina and the sarcolemma, suggesting that they might be activated satellite cells.

Finally, since therapeutic approaches for muscular dystrophy using rAAV vectors will likely reply upon systemic delivery protocols to target muscles bodywide,[14] we asked whether systemically injected mice would allow for satellite cell targeting. For this study, rAAV vectors expressing CMV-eGFP were retro-orbitally injected into wild-type mice. However, as with the intramuscular injections, no Pax7$^+$/eGFP$^+$ satellite cells were observed (Figure 8).

DISCUSSION

Dystrophic muscle is characterized by a chronic state of degenerative turnover. Cycles of degeneration and regeneration lead to a heterogeneous population of MPCs and regenerating myofibers in different stages of maturation. This diverse population represents a potential target for gene replacement strategies. rAAV6 is known to transduce skeletal muscle with high efficiency,[13,14,16] but transduction of MPCs and developing myofibers is less well-characterized. As rAAV6 is a candidate for treatment of genetic disorders of muscle, it is important that we possess a thorough knowledge of its transduction profile in myogenic cells. Thus, we evaluated both *in vitro* and *in vivo* rAAV6-mediated transduction of satellite cells, myoblasts, and developing myotubes and myofibers.

Our results demonstrate that rAAV6 preferentially targets myofibers and transduces myoblasts with reduced efficiency. This trend was apparent in both MM14 cells (Figure 1) and primary myogenic cultures (Figure 3). In a mixed population of mononuclear MPCs and developing myotubes, we observed a significant bias toward transduction of multinucleated muscle cells (Figure 3). Myoblast differentiation and myotube formation are complex processes governed by a number of transcriptional elements and regulatory factors (reviewed in Broek, *et al.* [35]). Myoblasts undergo extensive remodeling and reorganization as they fuse to form myotubes, and differentiation is accompanied by significant changes in extracellular matrix (ECM) composition and expression of cell-surface receptors.

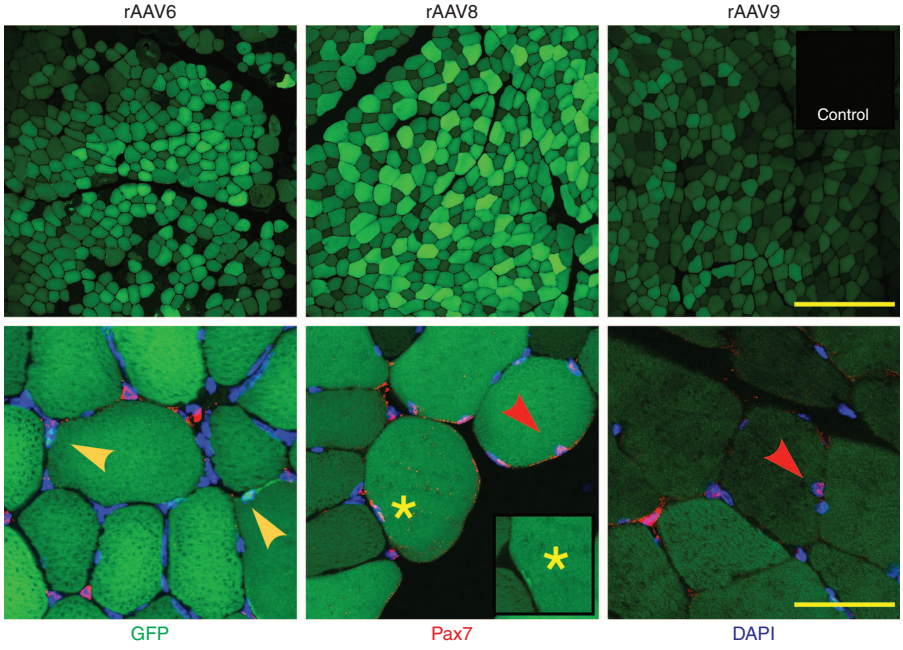

Figure 7 Comparison of rAAV6, 8, and 9 for satellite cell transduction. Eight-week-old C57Bl/6 mice were injected intramuscularly into the TA muscle with rAAV-CMV-eGFP vectors pseudotyped with either the serotype 6 (left panels), 8 (middle panels), or 9 (right panels) capsids. After 2 weeks, muscles were harvested, and cryosections were imaged for eGFP (top panels). The inset shows background eGFP fluorescence in uninjected muscles. Cryosections were also stained with DAPI, and immunostained with antibodies against laminin (not shown) and Pax7. Vector doses were adjusted to generate similar levels of transduction (rAAV6: 5×10^{10} vg; rAAV8 and 9: 2×10^{12} vg; $N = 4$ muscles each). As in the studies in Figure 6, no Pax7$^+$/eGFP$^+$ cells were observed following rAAV6 injection. However, a few rare instances were observed of cells between the basal lamina and the sarcolemma that were Pax7-negative/eGFP+ (bottom left panel, arrowheads). As with rAAV6, no Pax7$^+$/eGFP$^+$ cells were observed following rAAV9 injection (*e.g.*, bottom right panel, arrowhead points to a Pax7$^+$ satellite cell). In contrast, following injection of rAAV8 several Pax7$^+$/eGFP$^+$ cells were observed, but these represented less than 5% of the total Pax7$^+$ cells scored (bottom of middle panel, arrowhead; the positive satellite cell adjacent to the myofiber with the asterisk is shown in the inset minus the red (Pax7) fluorescence). Scale bars: 150 µm top; 30 µm bottom. DAPI, 4′,6-diamidino-2-phenylindole; eGFP, enhanced green fluorescent protein.

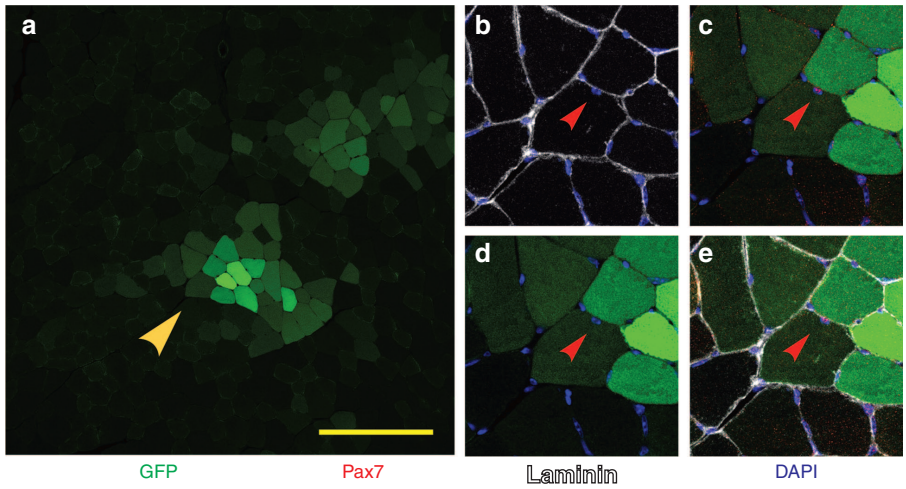

Figure 8 Analysis of satellite cell transduction following systemic injection of rAAV6. Four-week-old C57Bl/6 mice were retro-orbitally injected with 4×10^{12} vg of rAAV6-CMV-eGFP and analyzed 4 weeks later ($N = 4$ mice). (**a**) eGFP fluorescence in a cryosection of an isolated TA muscle showing transduced myofibers. (**b–e**) cryosections were stained with DAPI to visualize nuclei, and immunostainied with laminin and Pax7. An example of a $Pax7^+$/eGFP-negative satellite cell is shown. Laminin + DAPI imaging (**b**); Pax7 + DAPI + eGFP imaging (**c**); GFP + DAPI imaging (**d**); merge (**e**). The arrowhead points to a $Pax7^+$/eGFP-negative satellite cell. No $Pax7^+$/$eGFP^+$ cells were observed. Scale bars: 150 µm. DAPI, 4′,6-diamidino-2-phenylindole; eGFP, enhanced green fluorescent protein.

While the mechanisms regulating enhanced myofiber transduction remain unclear, these changes have the potential to influence tropism of rAAV6. We have previously demonstrated that heparin-binding capability in rAAV6 positively influences skeletal muscle transduction,[45] indicating that heparin interactions could differentially impact transduction efficiencies.

We also evaluated rAAV6 transduction efficiency in regenerating muscle (Figure 4). Though environmental factors *in vivo* are significantly more complex than *in vitro*, the results were generally consistent with our earlier findings. We observed a significant increase in transduction efficiency as the interval between notexin-injury and rAAV6-injection was increased. Notexin induces rapid necrosis of muscle fibers, but does not disrupt the basal lamina or promote satellite cell necrosis.[39]

Reduced transduction efficiency and clearance of vector at earlier rAAV6-injection timepoints may be influenced by a number of factors. Within 3–4 days postinjury, myoblasts begin to fuse and initiate formation of new myofibers.[34,40] Thus, the increase in transduction may simply reflect an increase in the percentage of available myofibers, which are more efficiently targeted by rAAV6. We did detect rare Pax7-negative cells under the basal lamina that had been transduced by rAAV6 vectors in some intramuscular injection studies, suggesting that activated satellite cells are able to be transduced *in vivo* following injury (Figure 7). However, rapid proliferation of satellite cells and myoblasts during the initial injury response may reduce transduction efficiency. As shown in Figure 2, proliferation and turnover negatively impacts transgene expression. Thus, it is conceivable that a substantial number of activated satellite cells and/or myoblasts transduced within the first few days of the injury response lose transgene expression during proliferation. Additionally, the inflammatory response to injury may increase clearance of vector.

Together our results indicate that rAAV6 does not effectively transduce satellite cells *in vivo*. All of the detection methods employed failed to obtain evidence of satellite cell transduction, with the exception of rare $Pax7^+$ cells transduced by rAAV8 (Figures 5–8; Supplementary Figure S1). It is unclear why quiescent satellite cells are not targeted by rAAV vectors. Skeletal muscle satellite cells reside in a quiescent state beneath the basal lamina until activated in response to muscle injury. It is possible that either the quiescent state of satellite cells or intrinsic features of the satellite cell niche limit transduction.

Our survey of rAAV-injected muscles was extensive, but the possibility exists that satellite cells were transduced at only a very low frequency, and were thus undetected by our methodologies. Nevertheless, a low level of satellite cell transduction is unlikely to be therapeutically relevant due to significant dilution and loss of vector genomes during the proliferative response. Since vector genomes remain primarily in an episomal state,[2] persistence of viral DNA and transgene expression is limited under conditions of high cellular turnover. Our analysis of reporter gene expression in rapidly proliferating C2C12 cells support this hypothesis (Figure 2). In addition, loss of vector genomes and transgene expression has been demonstrated in a model of partial hepatectomy.[4] Nakai *et al.* evaluated rAAV2 injection via portal vein, followed by partial hepatectomy. They observed a 92% reduction in vector genomes following liver regeneration. In contrast, transgene expression via a stably-integrated construct was unaffected by partial hepatectomy. Thus, as a nonintegrating vector, the persistence of rAAV *in vivo* is limited during tissue regeneration.

Our results also do not rule out the possibility that rAAV vectors may enter satellite cells and possibly express genes transiently before being lost. Such loss of vector would need to occur rapidly, as we did not detect vector genomes in freshly isolated satellite cells harvested 4 weeks after vector injection (Supplementary Figure S1), nor did we detect significant numbers of Pax7-positive satellite cells expressing vector-delivered transgene at 2 weeks postinjection (Figure 7). If even low levels of transgene expression could be obtained for short intervals then it might be possible to use genome editing strategies, such as Cas9/CRISPR or AAV-mediated homologous recombination to permanently modify the genome of muscle stem cells prior to vector loss.[46,47]

These data have implications for the design of future therapies, as a failure to deliver therapeutic genes to muscle stem cells indicates that any subsequent cycle of myofiber degeneration and regeneration would result in a loss of AAV genomes. It is unknown what the

half-life of a normal myofiber is in humans, but it seems reasonable to assume that such cells will display a low rate of turnover during normal activity. These results therefore suggest that readministration of vector will likely be necessary to maintain persistent transgene expression in skeletal muscles of dystrophic patients. However, the use of therapeutically protective constructs and other treatment strategies that reduce the rate of myofiber turnover or enhance muscle regeneration should effectively minimize the required frequency of vector readministration. Moreover, these results emphasize a niche for integrating vectors and cell-based therapies, and predict significant benefit from a combined therapeutic approach.

MATERIALS AND METHODS

Tissue culture

MM14 cells and C2C12 cells were cultured as previously described.[48] Cells were maintained at 37 °C in an atmosphere of 5% CO_2. C2C12 cells were transduced with rAAV6-CMV-βGal at an MOI of 100 and all timepoints were run in duplicate. MM14 cells were plated at 5×10^4 cells per well on 12-well plates and transduced with rAAV6-CMV-AP (3×10^9 vg per well) either 0, 5, or 10 days following induction of differentiation. Twelve wells were transduced per timepoint, and cells were harvested 3 days post-transduction for quantification of protein expression and vector genome copy number. Six of the 12 wells were independently analyzed for AP expression. For vector genome quantification, lysates from wells were combined in sets of two, for a total of $n = 3$ samples per timepoint. Experiments were repeated thrice.

Primary myoblasts were isolated, sorted, and cultured as previously described.[49] Briefly, TA muscles were digested in 0.2% collagenase II (Sigma-Aldrich, St Louis, MO) and filtered through 70 µm and then 40 µm filters (BD, San Diego, CA). Mononuclear cells were cultured on gelatin-coated plates with F10C media (Invitrogen, Carlsbad, CA) in the absence of FGF-2, to promote differentiation and myotube formation. Cultures were maintained for 4 days and GFP-expressing cells were tracked.

EDL myofibers were isolated and cultured as described.[33,50] The first day of fiber plating was designated as day 1. Three days after plating, cultures were switched to proliferation media for an additional 3 days. On day 7, cultures were switched to differentiation media. On the day that cultures were transduced, each well was administered 1×10^{11} vector genomes of AAV6-CMV-mCherry mixed into 50 µl of differentiation media. Vector was removed and media was exchanged for fresh media 16 hours post-transduction. Fibers were fixed 48 hours post-transduction, as described.[33]

Animal experiments

Animal studies were performed in accordance with the guidelines set forth by the University of Washington IACUC. All mice were bred on the C57Bl/6 background, in the University of Washington specific pathogen free barrier facility. All *in vivo* studies used mice that were between 8 and 12 weeks of age at the beginning of the experiment. For satellite cell transduction experiments, animals received bilateral IM injections of either rAAV6-CMV-mCherry (1×10^{10} vg per injection) or rAAV6-CMV-eGFP (1×10^{11} per injection; Figures 5 and 6) into the EDL or TA, respectively. rAAV6-CMV-mCherry was delivered to *mdx*:*Nestin-eGFP* ($n = 2$) and *wt*:*Nestin-eGFP* ($n = 2$) mice,[42] and rAAV6-CMV-eGFP was delivered to *wt* ($n = 4$) and *mdx* ($n = 2$) mice. At 4 weeks postinjection, mice were euthanized according to approved protocol, and muscles were harvested for single fiber cultures, primary myoblast cultures, or immunofluorescent staining. For *in vitro* transduction assays, fibers were collected from untreated *wt* (n=2) or *mdx* (n=2) EDL muscles, and an additional two *wt* mice were used as untreated controls for primary myoblast cultures. For the studies of multiple vector types (Figure 7), CMV-eGFP vectors pseudotyped with the AAV capsids for serotypes 6, 8, or 9 were injected at doses provided in the figure legends into C57Bl/6 mice ($N = 4$ per vector) and tissues were harvested after 2 weeks. For systemic injection (Figure 8), 4×10^{12} vg of rAAV6-CMV-eGFP was injected retro-orbitally into C57Bl/6 mice ($N = 4$) and tissues were harvested after 4 weeks.

For regeneration studies, wt mice ($n = 3$ muscles per timepoint) were given a IM injection of NTX (1 µg/ml; Sigma-Aldrich). Animals were then administered a second injection of rAAV6-CMV-AP (1×10^{10} vg per injection) on days 2, 3, 4, or 5 postinjury. Both injections were performed under isofluorane-induced anesthesia. At 2 weeks following rAAV6 injection, animals were euthanized according to approved protocol, and muscles were harvested for analysis.

Vector production

rAAV6 vectors were generated as previously described.[14] An Amersham AKTA10 HPLC machine (Amersham, Piscataway, NJ) was used for affinity purification on a HiTrap heparin column (Amersham). Southern analysis was utilized to determine the number of genome-containing particles in the vector preparation.

Luminometry assay

MM14 cells were harvested in 0.05% trypsin, 0.53 mmol/l ethylenediaminetetraacetic acid (Invitrogen). Cells were pelleted at ~2,000 × *g* and the supernatant was discarded. Cells were resuspended in tissue lysis buffer (0.5% sodium deoxycholate, 50 mmol/l Tris, 150 mmol/l NaCl, 1% Triton, 0.8% protease inhibitor cocktail (Sigma-Aldrich). Protein was quantified via spectrophotometric absorption using Bradford reagent (Peirce, Rockford, IL). The extract was then analyzed for alkaline phosphatase expression using a commercial luminometry kit (Applied Biosystems, Carlsbad, CA).

Vector genome quantification

Muscles were snap frozen in liquid nitrogen and then pulverized with a mortal and pestle. Pulverized muscle tissue was resuspended in tissue lysis buffer (0.5% Sodium deoxycholate, 50 mmol/l Tris, 150 mmol/l NaCl, 1% Triton, 0.8% protease inhibitor cocktail (Sigma-Aldrich). MM14 cell lysates were prepared as described above. DNA was isolated from cell and tissue lysates using a DNeasy blood and tissue kit (Qiagen, Valencia, CA) according the manufacturer's guidelines. Genome quantification was performed utilizing a SV40 polyadenylation site-specific probe and quantitative-PCR, as described.[14]

βGalactosidase staining

Media was aspirated and cells were fixed in 2% formaldehyde and 0.8% gluteraldehyde in phosphate-buffered saline (PBS) for 10 minutes at room temperature. Wells were then washed in cold PBS and incubated in staining solution (5 mmol/l K-ferricyanide, 5 mmol/l K-ferrocyanide, 2 mmol/l $MgCl_2$, and 4% Xgal in PBS) at 37 °C overnight.

Alkaline phosphatase staining

Muscle tissue was embedded in Tissue-Tek optimal cutting temperature medium (Sakura Finetek USA, Torrance, CA), rapidly frozen, and sectioned transversely. Sections were fixed with ice cold 4% paraformaldehyde, washed in cold PBS, placed in 65 °C phosphate-buffered saline for 90 minutes, rinsed in room temperature PBS, and washed in alkaline phosphatase buffer (0.1 mol/l Tris-HCl, 0.1 mol/l NaCl, 0.01 mol/l $MgCl_2$) for 10 minutes. Excess liquid was removed from the sections, and Sigma *FAST* BCIP/NBT substrate solution (Sigma-Aldrich) was applied to each section for 30 minutes at room temperature. Slides were rinsed in PBS, dehydrated in 70% ethanol (EtOH) for 5 minutes, 2× (95% EtOH for 2 minutes), 2× (100% EtOH for 2 minutes), 2× (xylene for 3 minutes), and cover-slipped with Permount mounting media (Fisher Scientific, Fair Lawn, NJ). Images were captured using Qlcam or Olympus digital cameras and processed using Qcapture Pro (Qimaging, British Columbia, Canada).

Satellite cell isolation

TA and EDL muscles were injected with rAAV6-CMV-mCherry in both legs for *wt* and *mdx* mice. Four weeks postinjection, injected muscles were dissected, minced, and subjected to collagenase II (Sigma #C6885) and Dispase (Worthington Biochemical, Lakewood, NJ) digestion. After repeated trituration and washes, cells were strained through 40 µmol/l filters (BD Biosciences, San Jose, CA). Filtered cells were incubated with rat anti-CD31, anti-CD45, anti-CD11b, and anti-Ly-6A/E (Sca-1) antibodies, all conjugated to biotin (Clones 390, 30-F11, M1/70, and D7, respectively; eBioscience, San Diego, CA). Cell suspension was then incubated with anti-biotin MicroBeads (MACS Miltenyi Biotec, Auburn, CA), washed, and then further purified by negative selection with magnetic affinity chromatography (MiniMACS Separator, MACS Miltenyi Biotec).

Immunofluorescent staining

Single fiber cultures were fixed for immunofluorescent staining as previously described.[33] Cultures were stained with mouse anti-desmin primary antibody (clone D33, at 1:100 dilution (Dako, Carpenteria, CA)) with goat anti-mouse Alexa Fluor 488 (Invitrogen) used as the secondary.

Muscles injected with rAAV6-CMV-GFP were excised and prepared for immunofluorescent staining as previously written.[42] Briefly, muscles were fixed in 4% paraformaldehyde and 1% sucrose for 2 hours, and were then successively immersed in 5, 10, and 20% sucrose for 30 minutes at each concentration. Muscles were then placed in 30% sucrose at 4 °C overnight and frozen in optimal cutting temperature for sectioning. For Pax7 staining, muscle cross-sections were incubated in citrate buffer (10 mmol/l citric acid monohydrate, 0.05% Tween 20, pH 6) for 15 minutes at 100 °C, washed with room temperature PBS, permeabilized for 10 minutes with 0.25% Triton-X in PBS, and washed again with room temperature PBS. Sections were then stained with a M.O.M. kit (Vector Labs, Burlingame, CA) following the manufacturer's instructions, using anti-Pax7 (Abcam 34360, San Francisco, CA), 1:200 for 1 hour, Alexa Fluor 594-streptavidin (Invitrogen), anti-alpha-2 laminin (Sigma-Aldrich L0663), and 4′,6-diamidino-2-phenylindole, 1:1,000 for 45 minutes. Images were captured using QIcam or Olympus digital cameras and processed using Qcapture Pro (Qimaging). The images in Figures 7 and 8 were acquired in the UW Biology Imaging Facility using a Leica TCS SPV II laser scanning confocal microscope (Leica-microsystems, Buffalo Grove, IL).

CONFLICT OF INTEREST

The authors declare no conflict of interest.

ACKNOWLEDGMENTS

The authors thank Eric Finn, James Allen, and Rainer Ng for assistance with vector production and titering, Lindsey Muir and Kristy Boyle for advice and assistance with cell culture, Scott Simpler, Ladan Mazzafarian, and Anastasia Vorontsova for help with animal husbandry, and Stephen Hauschka and En Kimura for assistance with primary myoblast cultures. A.A. was supported by the Medical Scientist Training Program, and Achievement Rewards for College Scientists, as well as a National Research Service Award (NIH F30NS068005). J.K.H. was supported by a NRSA T32 award from NIH. G.L.O. was supported by a Development grant from the Muscular Dystrophy Association (USA). Supported by NIH grants AR40864 and AG33610 (to J.S.C.).

REFERENCES

1. Smith, RH (2008). Adeno-associated virus integration: virus versus vector. *Gene Ther* **15**: 817–822.
2. Duan, D, Sharma, P, Yang, J, Yue, Y, Dudus, L, Zhang, Y *et al.* (1998). Circular intermediates of recombinant adeno-associated virus have defined structural characteristics responsible for long-term episomal persistence in muscle tissue. *J Virol* **72**: 8568–8577.
3. Schnepp, BC, Jensen, RL, Chen, CL, Johnson, PR and Clark, KR (2005). Characterization of adeno-associated virus genomes isolated from human tissues. *J Virol* **79**: 14793–14803.
4. Nakai, H, Yant, SR, Storm, TA, Fuess, S, Meuse, L and Kay, MA (2001). Extrachromosomal recombinant adeno-associated virus vector genomes are primarily responsible for stable liver transduction in vivo. *J Virol* **75**: 6969–6976.
5. Inagaki, K, Lewis, SM, Wu, X, Ma, C, Munroe, DJ, Fuess, S *et al.* (2007). DNA palindromes with a modest arm length of greater, similar 20 base pairs are a significant target for recombinant adeno-associated virus vector integration in the liver, muscles, and heart in mice. *J Virol* **81**: 11290–11303.
6. Schultz, BR and Chamberlain, JS (2008). Recombinant adeno-associated virus transduction and integration. *Mol Ther* **16**: 1189–1199.
7. Gao, GP, Alvira, MR, Wang, L, Calcedo, R, Johnston, J and Wilson, JM (2002). Novel adeno-associated viruses from rhesus monkeys as vectors for human gene therapy. *Proc Natl Acad Sci USA* **99**: 11854–11859.
8. Inagaki, K, Fuess, S, Storm, TA, Gibson, GA, Mctiernan, CF, Kay, MA *et al.* (2006). Robust systemic transduction with AAV9 vectors in mice: efficient global cardiac gene transfer superior to that of AAV8. *Mol Ther* **14**: 45–53.
9. Davidson, BL, Stein, CS, Heth, JA, Martins, I, Kotin, RM, Derksen, TA *et al.* (2000). Recombinant adeno-associated virus type 2, 4, and 5 vectors: transduction of variant cell types and regions in the mammalian central nervous system. *Proc Natl Acad Sci USA* **97**: 3428–3432.
10. Wang, C, Wang, CM, Clark, KR and Sferra, TJ (2003). Recombinant AAV serotype 1 transduction efficiency and tropism in the murine brain. *Gene Ther* **10**: 1528–1534.
11. Burger, C, Gorbatyuk, OS, Velardo, MJ, Peden, CS, Williams, P, Zolotukhin, S *et al.* (2004). Recombinant AAV viral vectors pseudotyped with viral capsids from serotypes 1, 2, and 5 display differential efficiency and cell tropism after delivery to different regions of the central nervous system. *Mol Ther* **10**: 302–317.
12. Alisky, JM, Hughes, SM, Sauter, SL, Jolly, D, Dubensky, TW Jr, Staber, PD *et al.* (2000). Transduction of murine cerebellar neurons with recombinant FIV and AAV5 vectors. *Neuroreport* **11**: 2669–2673.
13. Blankinship, MJ, Gregorevic, P, Allen, JM, Harper, SQ, Harper, H, Halbert, CL *et al.* (2004). Efficient transduction of skeletal muscle using vectors based on adeno-associated virus serotype 6. *Mol Ther* **10**: 671–678.
14. Gregorevic, P, Blankinship, MJ, Allen, JM, Crawford, RW, Meuse, L, Miller, DG *et al.* (2004). Systemic delivery of genes to striated muscles using adeno-associated viral vectors. *Nat Med* **10**: 828–834.
15. Zincarelli, C, Soltys, S, Rengo, G, Koch, WJ and Rabinowitz, JE (2010). Comparative cardiac gene delivery of adeno-associated virus serotypes 1-9 reveals that AAV6 mediates the most efficient transduction in mouse heart. *Clin Transl Sci* **3**: 81–89.
16. Zincarelli, C, Soltys, S, Rengo, G and Rabinowitz, JE (2008). Analysis of AAV serotypes 1-9 mediated gene expression and tropism in mice after systemic injection. *Mol Ther* **16**: 1073–1080.
17. Wang, Z, Zhu, T, Qiao, C, Zhou, L, Wang, B, Zhang, J *et al.* (2005). Adeno-associated virus serotype 8 efficiently delivers genes to muscle and heart. *Nat Biotechnol* **23**: 321–328.
18. Pacak, CA, Mah, CS, Thattaliyath, BD, Conlon, TJ, Lewis, MA, Cloutier, DE *et al.* (2006). Recombinant adeno-associated virus serotype 9 leads to preferential cardiac transduction in vivo. *Circ Res* **99**: e3–e9.
19. Chao, H, Liu, Y, Rabinowitz, J, Li, C, Samulski, RJ and Walsh, CE (2000). Several log increase in therapeutic transgene delivery by distinct adeno-associated viral serotype vectors. *Mol Ther* **2**: 619–623.
20. Emery, AE and Muntoni, F (2003). *Duchenne Muscular Dystrophy*. Oxford University Press: Oxford.
21. Chamberlain, J and Rando, T (2006). *Duchenne Muscular Dystrophy: Advances in Therapeutics*. Taylor and Francis: New York.
22. Brooks, SV and Faulkner, JA (1988). Contractile properties of skeletal muscles from young, adult and aged mice. *J Physiol* **404**: 71–82.
23. Cox, GA, Phelps, SF, Chapman, VM and Chamberlain, JS (1993). New mdx mutation disrupts expression of muscle and nonmuscle isoforms of dystrophin. *Nat Genet* **4**: 87–93.
24. Petrof, BJ, Shrager, JB, Stedman, HH, Kelly, AM and Sweeney, HL (1993). Dystrophin protects the sarcolemma from stresses developed during muscle contraction. *Proc Natl Acad Sci USA* **90**: 3710–3714.
25. Campbell, KP (1995). Three muscular dystrophies: loss of cytoskeleton-extracellular matrix linkage. *Cell* **80**: 675–679.
26. Banks, GB and Chamberlain, JS (2008). The value of mammalian models for duchenne muscular dystrophy in developing therapeutic strategies. *Curr Top Dev Biol* **84**: 431–453.
27. Olwin, BB and Rapraeger, A (1992). Repression of myogenic differentiation by aFGF, bFGF, and K-FGF is dependent on cellular heparan sulfate. *J Cell Biol* **118**: 631–639.
28. Templeton, TJ and Hauschka, SD (1992). FGF-mediated aspects of skeletal muscle growth and differentiation are controlled by a high affinity receptor, FGFR1. *Dev Biol* **154**: 169–181.
29. Motamed, K, Blake, DJ, Angello, JC, Allen, BL, Rapraeger, AC, Hauschka, SD *et al.* (2003). Fibroblast growth factor receptor-1 mediates the inhibition of endothelial cell proliferation and the promotion of skeletal myoblast differentiation by SPARC: a role for protein kinase A. *J Cell Biochem* **90**: 408–423.
30. Hannon, K, Kudla, AJ, McAvoy, MJ, Clase, KL and Olwin, BB (1996). Differentially expressed fibroblast growth factors regulate skeletal muscle development through autocrine and paracrine mechanisms. *J Cell Biol* **132**: 1151–1159.
31. Chamberlain, JS, Jaynes, JB and Hauschka, SD (1985). Regulation of creatine kinase induction in differentiating mouse myoblasts. *Mol Cell Biol* **5**: 484–492.
32. Bantel-Schaal, U, Braspenning-Wesch, I and Kartenbeck, J (2009). Adeno-associated virus type 5 exploits two different entry pathways in human embryo fibroblasts. *J Gen Virol* **90**(Pt 2): 317–322.
33. Shefer, G and Yablonka-Reuveni, Z (2005). Isolation and culture of skeletal muscle myofibers as a means to analyze satellite cells. *Methods Mol Biol* **290**: 281–304.
34. Wallace, GQ and McNally, EM (2009). Mechanisms of muscle degeneration, regeneration, and repair in the muscular dystrophies. *Annu Rev Physiol* **71**: 37–57.
35. Ten Broek, RW, Grefte, S and Von den Hoff, JW (2010). Regulatory factors and cell populations involved in skeletal muscle regeneration. *J Cell Physiol* **224**: 7–16.
36. Villalta, SA, Nguyen, HX, Deng, B, Gotoh, T and Tidball, JG (2009). Shifts in macrophage phenotypes and macrophage competition for arginine metabolism affect the severity of muscle pathology in muscular dystrophy. *Hum Mol Genet* **18**: 482–496.
37. Brunelli, S and Rovere-Querini, P (2008). The immune system and the repair of skeletal muscle. *Pharmacol Res* **58**: 117–121.
38. Tidball, JG and Villalta, SA (2010). Regulatory interactions between muscle and the immune system during muscle regeneration. *Am J Physiol Regul Integr Comp Physiol* **298**: R1173–R1187.

39. Plant, DR, Colarossi, FE and Lynch, GS (2006). Notexin causes greater myotoxic damage and slower functional repair in mouse skeletal muscles than bupivacaine. *Muscle Nerve* **34**: 577–585.
40. Lefaucheur, JP and Sébille, A (1995). The cellular events of injured muscle regeneration depend on the nature of the injury. *Neuromuscul Disord* **5**: 501–509.
41. Yablonka-Reuveni, Z, Day, K, Vine, A and Shefer, G (2008). Defining the transcriptional signature of skeletal muscle stem cells. *J Anim Sci* **86**(14 Suppl): E207–E216.
42. Day, K, Shefer, G, Richardson, JB, Enikolopov, G and Yablonka-Reuveni, Z (2007). Nestin-GFP reporter expression defines the quiescent state of skeletal muscle satellite cells. *Dev Biol* **304**: 246–259.
43. Kuang, S and Rudnicki, MA (2008). The emerging biology of satellite cells and their therapeutic potential. *Trends Mol Med* **14**: 82–91.
44. Brack, AS, Conboy, IM, Conboy, MJ, Shen, J and Rando, TA (2008). A temporal switch from notch to Wnt signaling in muscle stem cells is necessary for normal adult myogenesis. *Cell Stem Cell* **2**: 50–59.
45. Arnett, AL, Beutler, LR, Quintana, A, Allen, J, Finn, E, Palmiter, RD *et al.* (2013). Heparin-binding correlates with increased efficiency of AAV1- and AAV6-mediated transduction of striated muscle, but negatively impacts CNS transduction. *Gene Ther* **20**: 497–503.
46. Chamberlain, JR, Schwarze, U, Wang, PR, Hirata, RK, Hankenson, KD, Pace, JM *et al.* (2004). Gene targeting in stem cells from individuals with osteogenesis imperfecta. *Science* **303**: 1198–1201.
47. Hsu, PD, Lander, ES and Zhang, F (2014). Development and applications of CRISPR-Cas9 for genome engineering. *Cell* **157**: 1262–1278.
48. Olwin, BB and Hauschka, SD (1988). Cell surface fibroblast growth factor and epidermal growth factor receptors are permanently lost during skeletal muscle terminal differentiation in culture. *J Cell Biol* **107**: 761–769.
49. Kimura, E, Han, JJ, Li, S, Fall, B, Ra, J, Haraguchi, M *et al.* (2008). Cell-lineage regulated myogenesis for dystrophin replacement: a novel therapeutic approach for treatment of muscular dystrophy. *Hum Mol Genet* **17**: 2507–2517.
50. Rosenblatt, JD, Lunt, AI, Parry, DJ and Partridge, TA (1995). Culturing satellite cells from living single muscle fiber explants. *In Vitro Cell Dev Biol Anim* **31**: 773–779.

Supplementary Information accompanies this paper on the *Molecular Therapy—Methods & Clinical Development* website (http://www.nature.com/mtm)